DOWNSCALING OCEAN SURFACE NET RADIATION AT GLOBAL SCALES WITH RANDOM FOREST

Jianglei Xu[a,b] *, Bo Jiang*[a,b*]

[a]State Key Laboratory of Remote Sensing Science, Jointly Sponsored by Beijing Normal University and Institute of Remote Sensing and Digital Earth of Chinese Academy of Sciences, Beijing 100875
[b]Institute of Remote Sensing Science and Engineering, Faculty of Geographical Science, Beijing Normal University, Beijing 100875, China
*Corresponding author. E-mail: bojiang@bnu.edu.cn

ABSTRACT

The ocean surface net radiation (R_n) characterizing the ocean surface radiation budget, is a key variable of interest in ocean climate modeling and analysis, which determines the climate model of ocean surface with heat, freshwater and momentum flux. Most available ocean surface R_n data face various issues in accuracy, spatiotemporal patterns, and coarse spatial resolutions. J-OFURO3 (The third generation of Japanese Ocean Flux Datasets with Use of Remote Sensing Observations) released recently is considered to be one of the best datasets in ocean R_n, but its spatial resolution is also at 0.25°. In this study, we downscaled ocean surface R_n from J-OFURO3 using AVHRR TOA observations with Random Forest (RF) method. The accuracy of the downscaling daily surface ocean R_n is satisfactory with a root mean square error (RMSE) of 29Wm^{-2}, which is better than other reanalysis data and comparable to that of CERES-SYN.

Index Terms— Ocean surface net radiation, downscaling, AVHRR TOA Observations, Random Forest

1. INTRODUCTION

The surface radiation is characterized by the net radiation (R_n) at the Earth's ocean and land surface[1]. Surface R_n is the difference between the downward and upward radiations across the shortwave (0.3-3.0um) and longwave spectrum (3.0-100.0um). Compared with land surface R_n, the study of ocean surface R_n is relatively rare. However, ocean covers about two thirds of the globe and plays an important role in the climate system. The oceans are a source of atmospheric moisture, which control air-sea exchange of heat and store it at various depths in the oceans[2]. Besides geographical locations, two factors, affecting ocean heat flux balance, are absorption of shortwave radiation (warming ocean surface) and emission of longwave radiation (cooling ocean surface)[3, 4], which are the main components of R_n. The R_n, together with the fluxes of sensible and latent heat, in turns, affect the climatic state of both the atmosphere and ocean[5]. Meanwhile, ocean surface R_n is an important input variable in most air-sea interactions models, which largely influence the performance of these models[6]. Thus, studying ocean surface R_n is essential for analysis of ocean climate system.

Ocean surface R_n could be obtained from various sources, including in-situ measurements, satellite product, reanalysis data, hybrid data and ship-based estimations. In-situ measurements from buoy or instruments have the highest accuracy and are often used to evaluate other ocean R_n data[7]. But such data is spatially sparely distributed and has a short time frame, so that they cannot be suitable for characterizing ocean surface R_n at large spatial scale. Several studied indicated that the accuracy of satellite-based ocean surface R_n is usually better than that from reanalysis data, though satellite-based data has the short time period and coarse spatial resolution [8]. Meanwhile, the hybrid data and ship-based estimations also have the similar issues in the field of accuracy, spatial and temporal resolution[9].

Among these products, J-OFURO3 (The third generation of Japanese Ocean Flux Datasets with Use of Remote Sensing Observations) is currently optimal in accuracy and spatial resolution with a spatial resolution of 0.25° from 1988-2013. In this study, we validated the accuracy of J-OFURO3 in ocean surface R_n and found that the validation results of J-OFURO3 in ocean surface R_n is even better than CERES. For obtaining the ocean surface R_n in a finer spatial resolution, we proposed a statistical method to downscale J-OFURO3 ocean surface R_n data by using the AVHRR data in this study.

2. DATA

In situ observations from six networks were collected. The information of the six networks are provided in Table I. The sites are distributed over global ocean, as shown in Fig.1.

J-OFURO3 daily ocean radiation products are generated from ISCCP and CERES by re-gridding method

and SST (sea surface temperature) data with a spatial resolution of 0.25° from 1988 to 2013[10]. This dataset is available at https://j-ofuro.scc.u-tokai.ac.jp/. CERES-SYN radiation data at 1° was also used in this study, its radiation components were calculated by radiation transfer model[11] (https://ceres.larc.nasa.gov/).

Table I Metadata for six networks used in this study

Abbreviation	Site number	URL
PIRATA	7	http://www.pmel.noaa.gov/
RAMA	6	http://www.pmel.noaa.gov/
TAO	15	http://www.pmel.noaa.gov/
UOP	30	http://uop.whoi.edu/index.html
OS	12	https://dods.ndbc.noaa.gov/oceansites/
CNNADC	3	http://www.chinare.org.cn/

The AVHRR TOA reflectance and bright temperature data (AVH02C1) used in this study were obtained from Version 5 of the land Long-Term Data Record (LTDR, http://ltdr.nascom.nasa.gov/) project. The project provided a consistent AVHRR dataset at a spatial resolution of 0.05°, from 1981 to the present[12], based on GAC (Global Area Cover) data from AVHRR sensors, and the corresponding angle information (solar zenith angle, view zenith angle, and relative azimuth angle) and cloud information were also used.

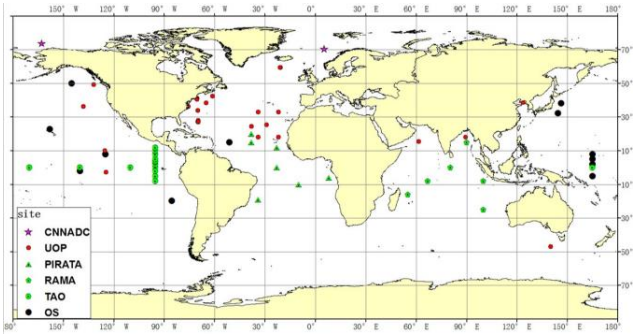

Fig.1. Global ocean distribution of six networks

3. METHOD

The entire downscaling procedure (see Fig.2) includes six parts: (1) High-quality sample determine. Taking the CERES as the reference, the J-OFURO3 was aggregated into 1° to compare with the CERES in ocean surface R_n, and the high-quality J-OFURO3 pixels were selected according to several criterions. (2) AVHRR data extraction. The AVHRR windows (5*5 for each) were extracted based on each high-quality J-OFURO3 sample (0.25°), and then a consistency check was implemented for each AVHRR pixel in these windows for quality control. (3) Downscaling method development. Establishing the statistical relationships between the AVHRR data (by averaging each AVHRR window) and J-OFURO3 high quality ocean surface R_n samples with RF method under clear and cloud sky conditions. (4) Ocean surface R_n_AVHRR generation. With the AVHRR inputs, the downscaled ocean surface R_n_AVHRR was generated at 0.05°. (5) Residual correction. To achieve a high accuracy downscaled ocean surface R_n, a simple residual correction was conducted. (6) Validation. The final R_n_AVHRR data was validated against the in-situ measurement.

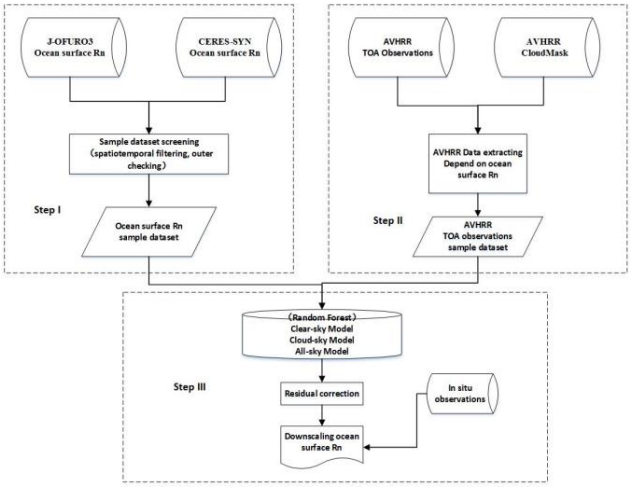

Fig. 2. The flowchart of downscaling J-OFURO3 ocean surface R_n

4. RESULT

4.1. High-quality J-OFURO3 R_n determine

Figure3 gives the multi-year average difference distribution between CERES-SYN and J-OFURO3 in ocean R_n, and its corresponding histogram.

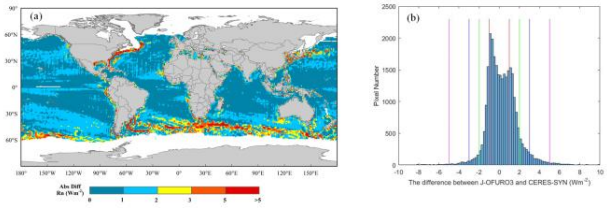

Fig. 3. Result of spatial difference analysis, (a) is absolute difference distribution map, (b) is corresponding histogram between these two products.

Based on the comparison results, 1 Wm^{-2} was selected as the threshold to determine the high-quality samples, which means that a pixel (1°) from the aggregated J-OFURO3 would be selected as long as its difference with the corresponding CERES pixel is less than 1 Wm^{-2}. Moreover, the spatial distribution and the total amount of samples were also considered. Finally, 6101 sample points were determined, and their spatial distribution is shown in Fig.4.

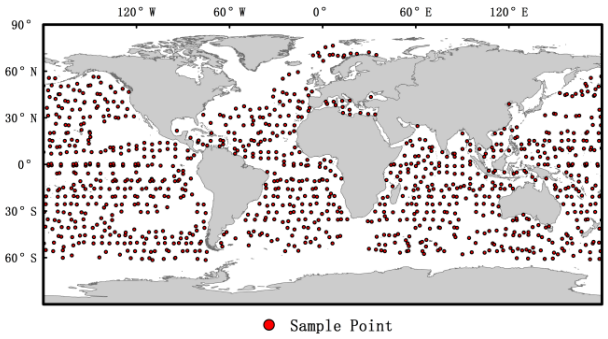

Fig. 4. High quality sample points distribution map

4.2. Ocean surface R_n downscaling

4.2.1 Downscaling algorithm development

The statistical model was developed between AVHRR data and the samples by using RF model. The inputs include 5 AVHRR TOA observations and 3 angle information, and the cloud mask was used to determine the clear or cloudy sky. The samples during 2003-2005 were used as the training data, and the samples in 2006 were taken as the test dataset. Figure5 shows the RF algorithm performances in downscaling J-OFURO3 ocean surface R_n under clear, cloud and all-sky conditions. It could be concluded that the RF has the best performance under clear sky, but the result under all-sky is also acceptable.

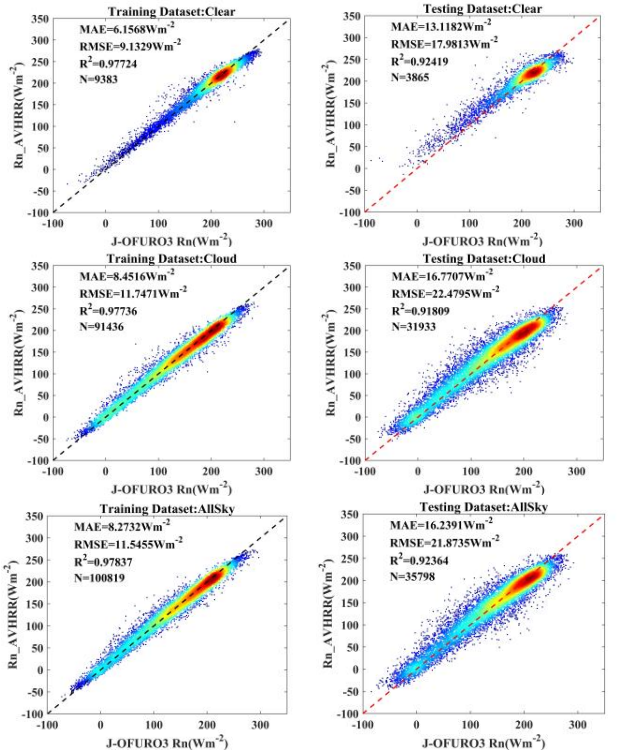

Fig. 5. Scatter plots of RF training and validation results. The plots in the left column are training results and the right one are validation results. There are clear, cloud and all sky conditions from top to bottom.

4.2.2 Validation with in-situ measurement

RF algorithm under all-sky condition was used to generate the ocean surface R_n based on AVHRR (R_n_AVHRR), and the accuracy of R_n_AVHRR was validated against in-situ observations. Figure6 shows the validation results in ocean surface between in-situ observations and R_n_AVHRR with a RMSE of 29.03 Wm^{-2}, MAE of 2.57Wm^{-2}, and R^2 of 0.82. The accuracy of the R_n_AVHRR is satisfactory.

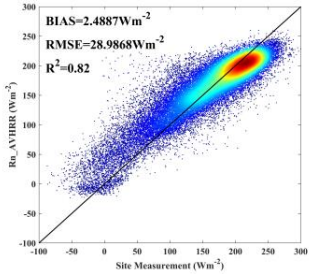

Fig. 6. Scatter of validation results with In-situ measurements.

Fig.7 gives the time series of R_n_AVHRR, J-OFURO3 and buoy measurements at two sites of OS_NTAS (15°N, 51°W) and OS_STRTATUS (19.75°S, 88.33°W). The variations of R_n_AVHRR are consistent with the other two datasets, but it has the tendency to underestimate the large Rn values and overestimate the small R_n values.

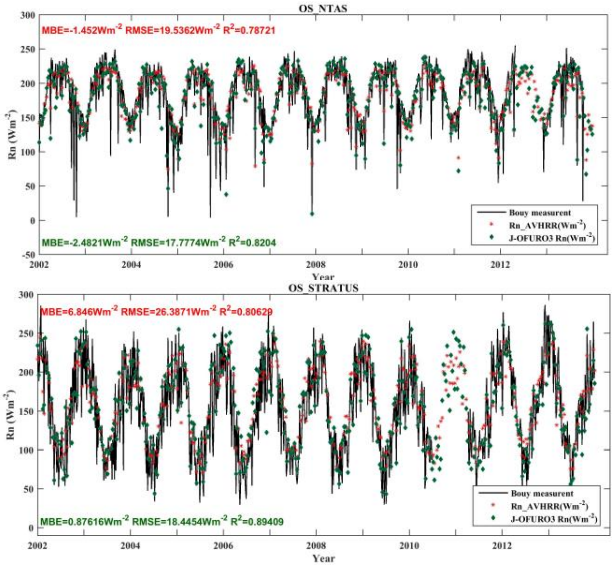

Fig. 7. Time series of Rn_AVHRR (red asterisk), J-OFURO3 (green diamond) and observations (black line) from two sites: OS_NTAS (15°N, 51°W) and OS_STRATUS (19.75°S, 88.33°W)

4.2.3 Residual correction

The residual between R_n_AVHRR and J-OFURO3 values cannot be ignored. The residual correction procedure consists of three steps: The first, re-aggregate R_n_AVHRR into 0.25°. Secondly, calculate the ocean surface R_n residuals between the aggregated R_n_AVHRR and the corresponding J-OFURO3. Third, correct the R_n_AVHRR by adding the calculated residuals. Fig.8 shows the R_n_AVHRR after residual correction. Obviously, the

discrepancies of the two datasets (R_n_AVHRR and J-OFURO3) are reduced after residual correction.

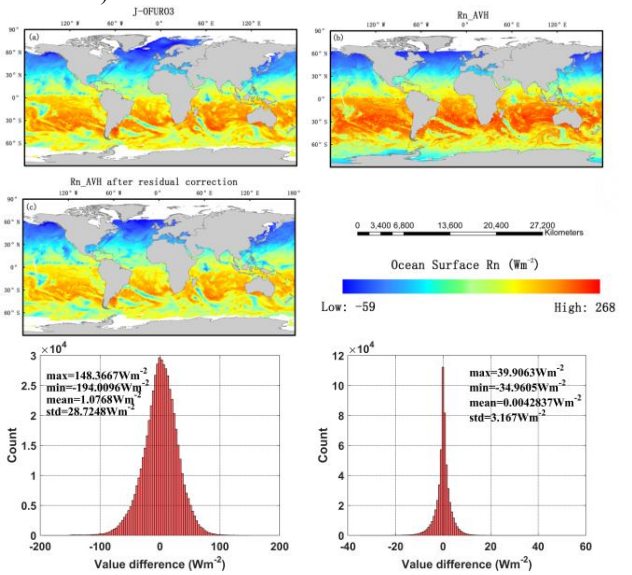

Fig. 8. The result of residual correction: (a) is J-OFURO3 R_n, (b) is original R_n_AVHRR and (c) is R_n_AVHRR after correction. The left difference histogram is between J-OFURO3 and original R_n_AVHRR and the right difference histogram is between J-OFURO3 and R_n_AVHRR after correction.

5. CONCLUSION

Ocean surface R_n with high spatial resolution is essential for climatic research and air-sea interaction model forcing. However, the spatial resolution of most ocean surface R_n products are at degree scales that hardly meet the needs of ocean climate studies and applications. In this study, we proposed a downscaling algorithm to downscale the J-OFURO3 ocean surface R_n from 0.25° to 0.05° based on AVHRR data with random forest method. The validation results of the downscaled R_n_AVHRR are satisfactory with a RMSE of 29.03 Wm^{-2}, MAE of 2.57Wm^{-2}, and R^2 of 0.82. After residual correction, the quality of the final Rn_AVHRR has been improved significantly.

However, the developed algorithm still has the tendency to underestimate the large ocean surface R_n values and overestimate the small R_n values, thus, more efforts would be made to improve this study in the near future.

6. ACKNOWLEDGMENT

This study was funded by the Chinese Grand Research Program on Climate Change and Response under the projects 2016YFA0600101. We thank the PIRATA, RAMA, TAO, UOP, OS, CNNADC networks for offering the filed measurements of flux variables. We would also thank the reviewers for their valuable comments, which greatly improved the quality of this manuscript.

7. REFERENCES

[1] K. E. Trenberth, J. T. Fasullo, and J. Kiehl, "Earth's global energy budget," *Bulletin of the American Meteorological Society,* vol. 90, pp. 311-324, 2009.

[2] L. Yu, K. Haines, M. Bourassa, M. Cronin, S. Gulev, S. Josey, *et al.*, "Towards achieving global closure of ocean heat and freshwater budgets: Recommendations for advancing research in air-sea fluxes through collaborative activities," in *Report of the CLIVAR/GSOP/WHOI Workshop on Ocean Syntheses and Surface Flux*, 2013.

[3] Y. E. Nanshan and Y. E. Fang, "Solar Radiation Heat Transfer of Air Conditioning and Refrigeration Technology," *Refrigeration,* 2012.

[4] J. Carter Ohlmann, D. A. Siegel, and C. Gautier, "Ocean Mixed Layer Radiant Heating and Solar Penetration: A Global Analysis," *Journal of Climate,* vol. 9, pp. 2265-2280, 1996.

[5] H. D. Behr, "Net Total Radiation at the Sea Surface of the Atlantic Ocean between 30°N and 30°S," vol. 26, pp. 349-55, 1990.

[6] D. I. Berry and E. C. Kent, "Air–Sea fluxes from ICOADS: the construction of a new gridded dataset with uncertainty estimates," 2011.

[7] C.-C. Chan and J.-S. Hwang, "Site Representativeness of Urban Air Monitoring Stations," *Journal of the Air & Waste Management Association,* 1996.

[8] A. Jia, S. Liang, B. Jiang, X. Zhang, and G. Wang, "Comprehensive Assessment of Global Surface Net Radiation Products and Uncertainty Analysis," *Journal of Geophysical Research: Atmospheres,* 2017.

[9] B. P. Kumar, J. Vialard, M. Lengaigne, V. S. N. Murty, and M. J. Mcphaden, "TropFlux: air-sea fluxes for the global tropical oceans—description and evaluation," *Climate Dynamics,* vol. 38, pp. 1521-1543, 2012.

[10] H. Tomita, T. Hihara, S. I. Kako, M. Kubota, and K. Kutsuwada, "An introduction to J-OFURO3, a third-generation Japanese ocean flux data set using remote-sensing observations," *Journal of Oceanography,* pp. 1-24, 2018.

[11] S. K. Gupta, C. H. Whitlock, N. A. Ritchey, and A. C. Wilber, "Clouds and the Earth's Radiant Energy System (CERES) Algorithm Theoretical Basis Document," *An Algorithm for Longwave Surface Radiation Budget for Total Skies (Subsystem 4.6. 3), Release,* vol. 2, 1997.

[12] J. Pedelty, S. Devadiga, E. Masuoka, M. Brown, J. Pinzon, C. Tucker, *et al.*, "Generating a long-term land data record from the AVHRR and MODIS instruments," in *Geoscience and Remote Sensing Symposium, 2007. IGARSS 2007. IEEE International*, 2007, pp. 1021-1025.